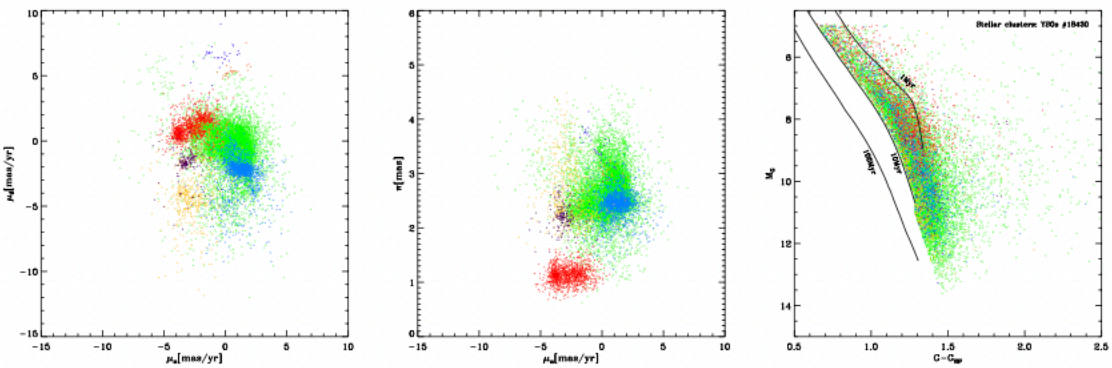

Fig. C.4. Proper motions in RA and Dec, parallaxes, and CAMDs of the YSOs associated with the Orion complex. The symbol colours of the sub-clusters are the same as in Fig. C.3. Three representative solar metallicity isochrones from the Pisa models are also shown.

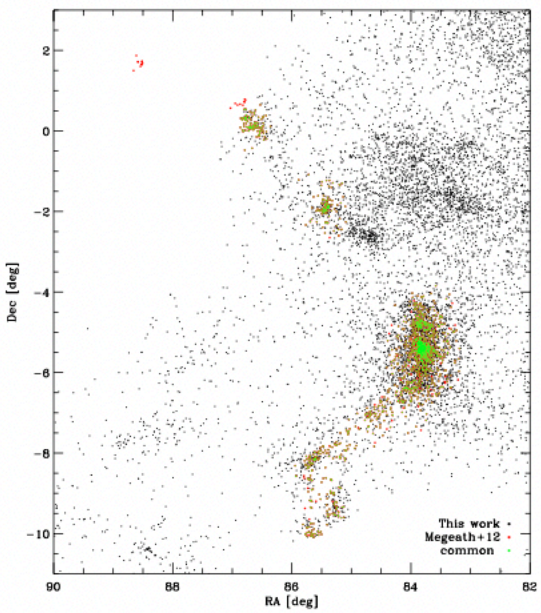

Fig. C.5. Spatial distribution of Orion YSOs compared to YSOs found in Megeath et al. (2012), indicated as black and red symbols, respectively. YSOs in common to the two catalogues are drawn as green symbols.

C.3. Interstellar dust-free SFR NGC 2362

At a distance of 1 354±192 pc, NGC 2362 is an SFR characterised by a very low and uniform reddening, estimated to be E(B-V)=0.1 (Moitinho et al. 2001). For this reason, the cluster shows a small spread in the optical V versus V-I diagram, as found by Moitinho et al. (2001) and confirmed by Damiani et al. (2006). This enables us to constrain the duration of the star formation process that in this region has been about 1-2 Myr (Damiani et al. 2006). This result was derived on the basis of a Chandra-ACIS X-ray observation, pointed towards the cluster, from which a list of very likely members has been obtained. As for the case of NGC 2264, this cluster was found using our procedure in a region more extended than that investigated by Damiani et al. (2006). The 879 YSOs compatible with being members of NGC 2362 are plotted in Fig. C.6. Within the nominal cluster centre, l=238.2°, -5.54° (Damiani et al. 2006), we found 150 candidate members, while the others are mostly concentrated around the three bumps visible in the IR image. A further sub-group of cluster members shows an aligned spatial distribution roughly going from NGC 2362 to the H II region LBN 1059.

To compare our data with the list of 387 X-ray members by Damiani et al. (2006), we cross-matched this list with the *Gaia* EDR3 catalogue, using the cross-match service provided by CDS, Strasbourg and adopting a matching radius of 0.5″. We find that 294 of them have a single *Gaia* EDR3 counterpart, but 129 are compliant with our initial data set restrictions and fall in the PMS region of the CAMD compatible with ages < 10 Myr. Among these, 118 (i.e. ∼ 91%) are in common with our list of YSOs. This fraction confirms that, even though our list of YSOs is incomplete due to the significant fraction of members discarded, a priori, with the adopted data restrictions and in the adopted photometric ranges, the efficiency of our method in detecting very likely members is very high. This is notably true if we consider that X-ray detections select YSOs without any bias based on the stellar evolutionary status (Class II or III YSOs) and do so with a high degree of efficiency in the spectral types (G to M) we are working on.

Within the Chandra-ACIS field of view, we selected a total of 150 YSOs, and 32 of them (21%) are not X-ray detected. X-ray detections found in Damiani et al. (2006) are complete for masses larger than 0.4 $M_\odot$, which, assuming the cluster age of 4-5 Myr (Mayne & Naylor 2008), corresponds to $M_G \simeq 7.5$. By considering that more than 50% of these X-ray-undetected YSOs are fainter than this limit and that most of them are located far from the cluster centre, where the Chandra-ACIS spatial resolution is lower, we are confident that the 32 X-ray-undetected YSOs classified by us are likely members.

As for the other clusters, we investigated proper motions, parallaxes, and CAMD, which are shown in Fig. C.7. The proper motion scatter plot indicates that the distribution of YSOs falling in the Chandra-ACIS is actually more concentrated than that of the overall cluster, which shows an inclined trend. This confirms that the entire cluster is characterised by a kinematic structure slightly more complex than that of the sub-group of YSOs falling